Supplementary Figures

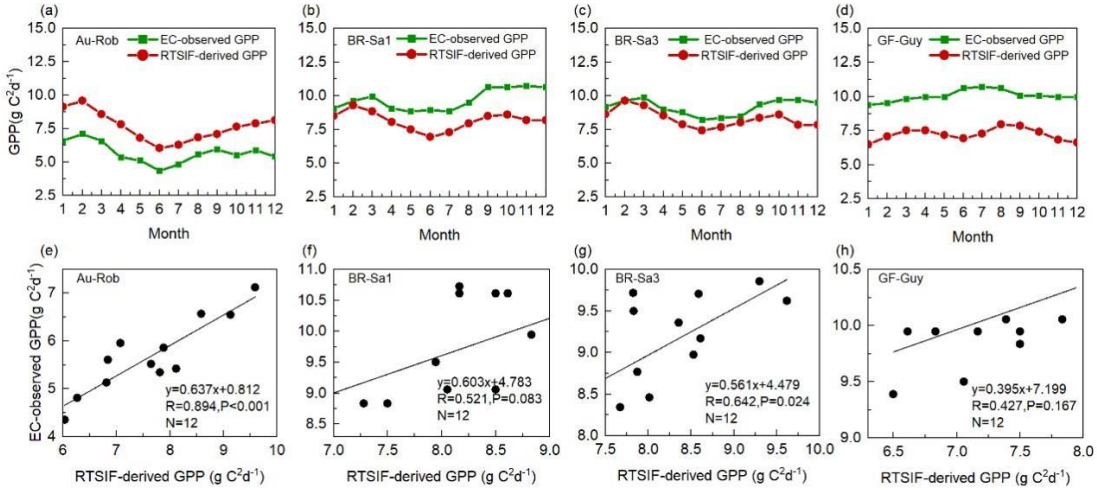

Figure S1. Comparisons between monthly RTSIF-derived GPP (red) and observed GPP at eddy covariance (EC) tower sites (green). (a, e) Au-Rob, (b, f) BR-Sa1, (c, g) BR-Sa3, and (d, h) GF-Guy.

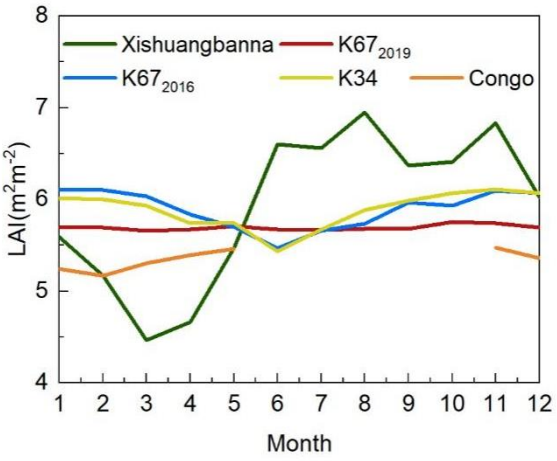

Figure S2. The seasonality of observed total LAI values from previously published literatures.

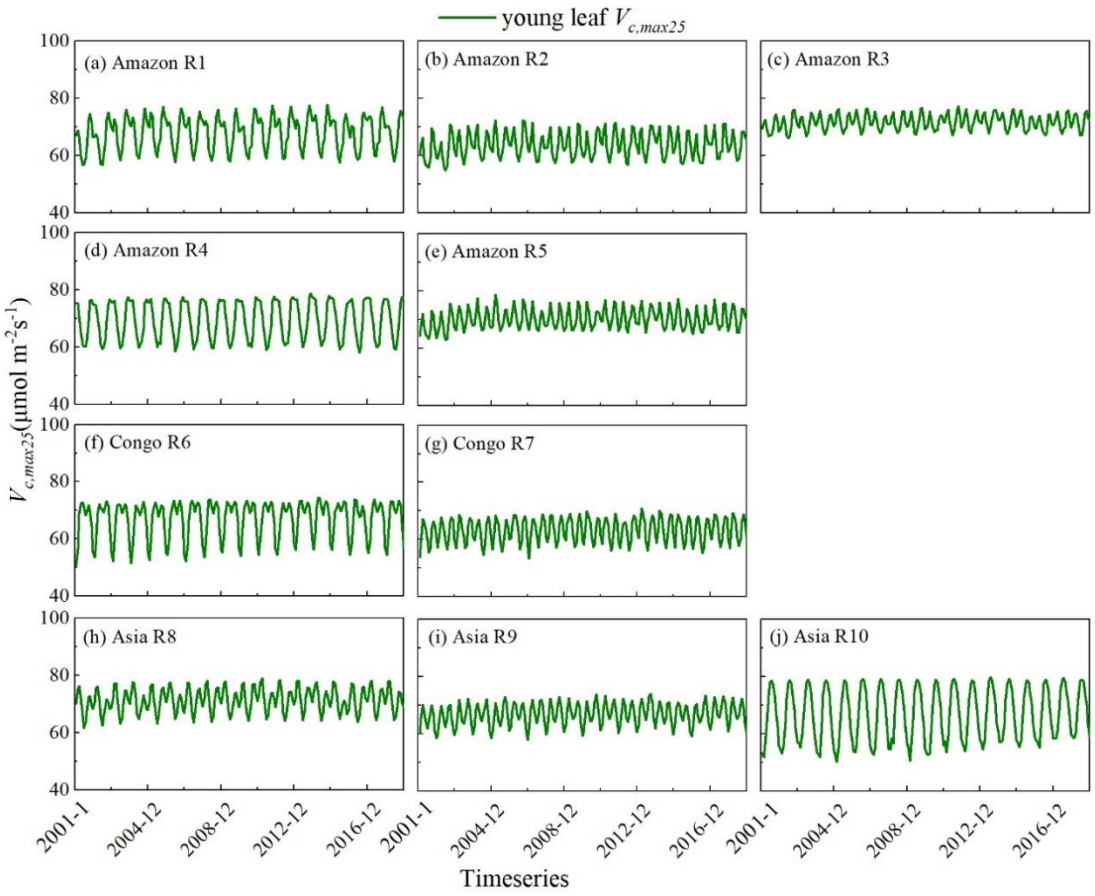

Figure S3. Time series of the simulated young leaf $V_{c,max25}$ in ten subzones clustered according to the K-means analysis.

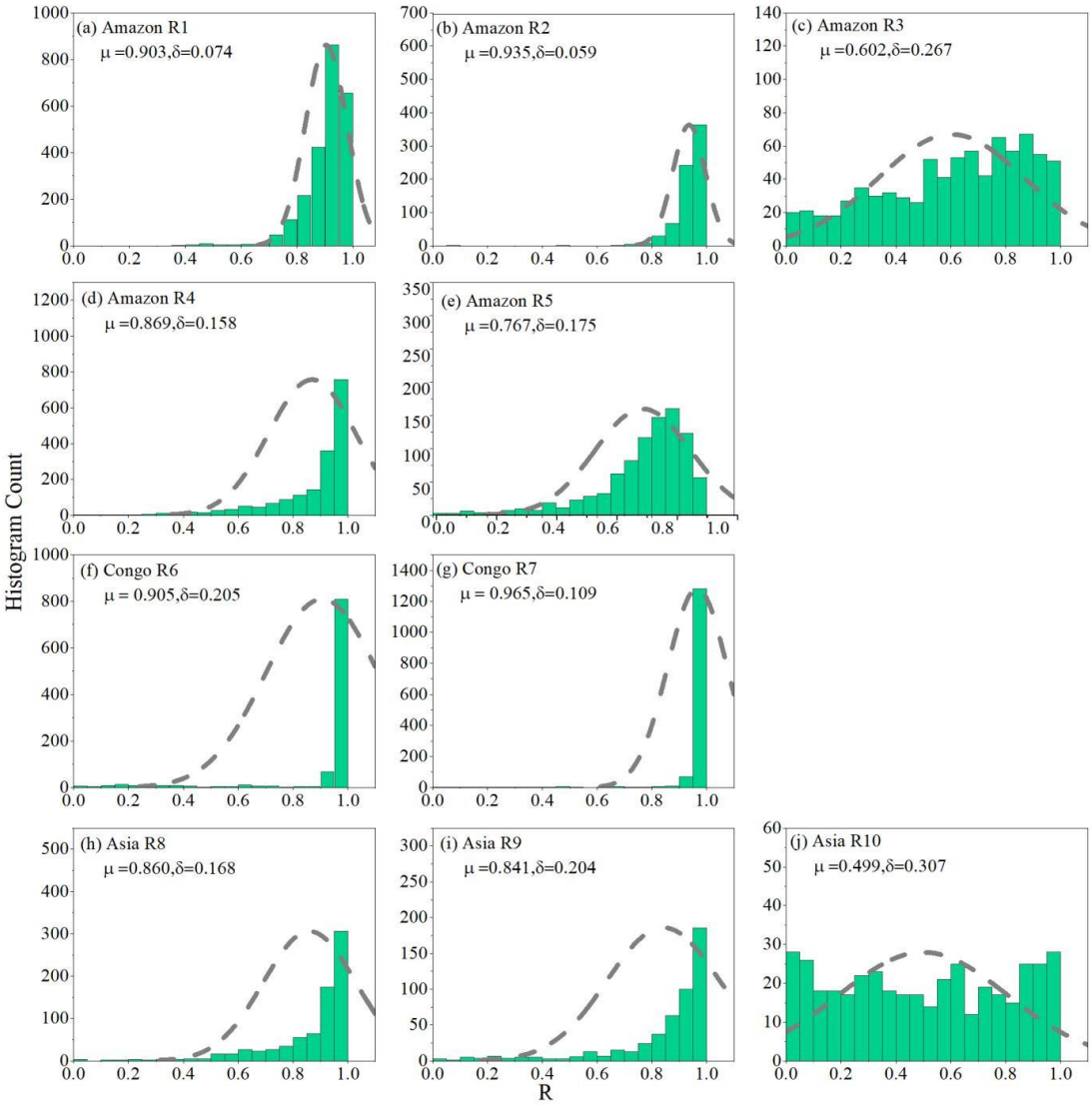

Figure S4. Statistical analyses of R between SIF-simulated monthly $V_{c,max25}$ and dissolved $V_{c,max25}$ from GPP for the ten k-mean clustered subzones

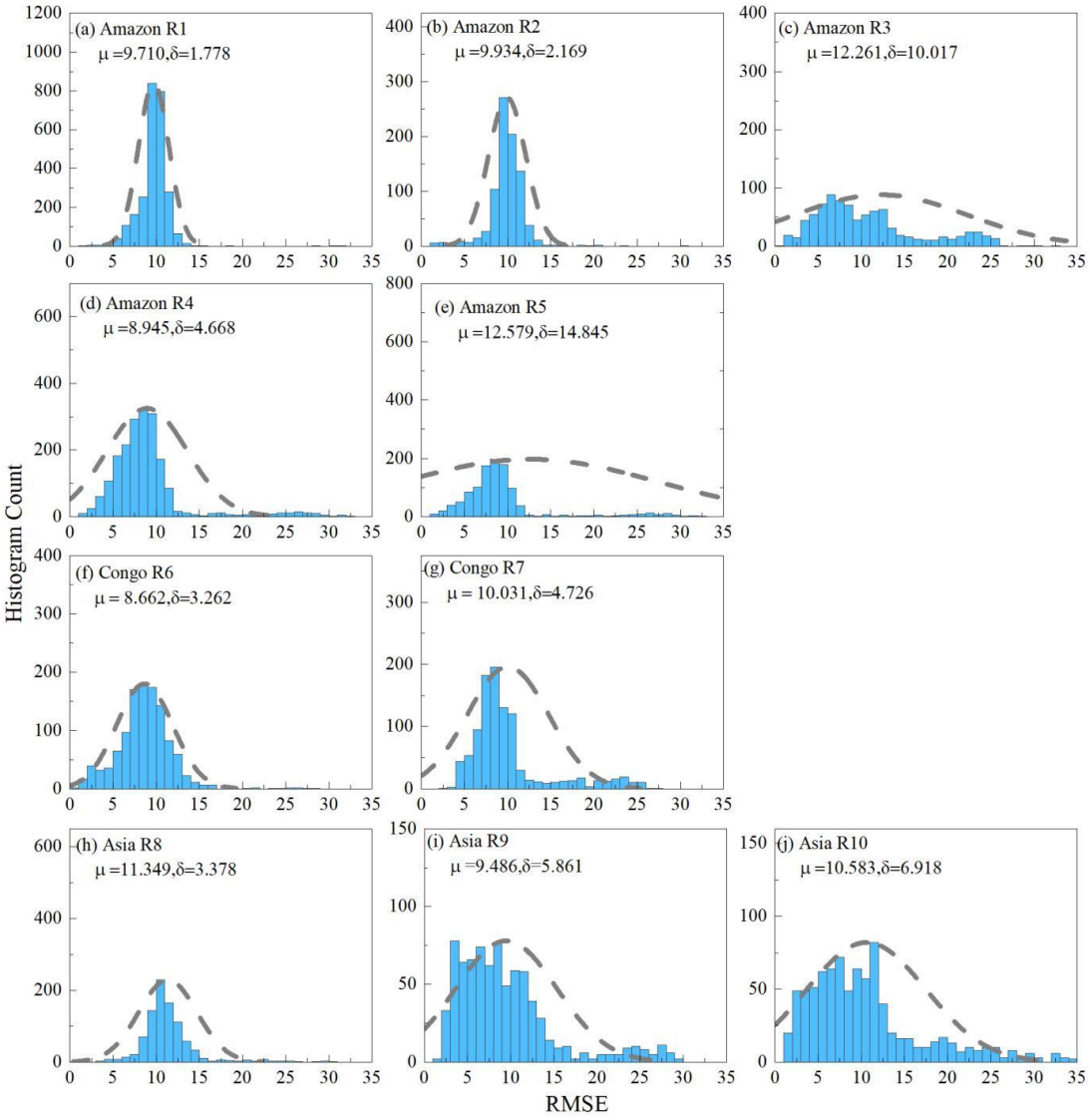

Figure S5. Statistical analyses of RMSE between SIF-simulated monthly $V_{c,max25}$ and dissolved $V_{c,max25}$ from GPP for the ten K-means clustered subzones

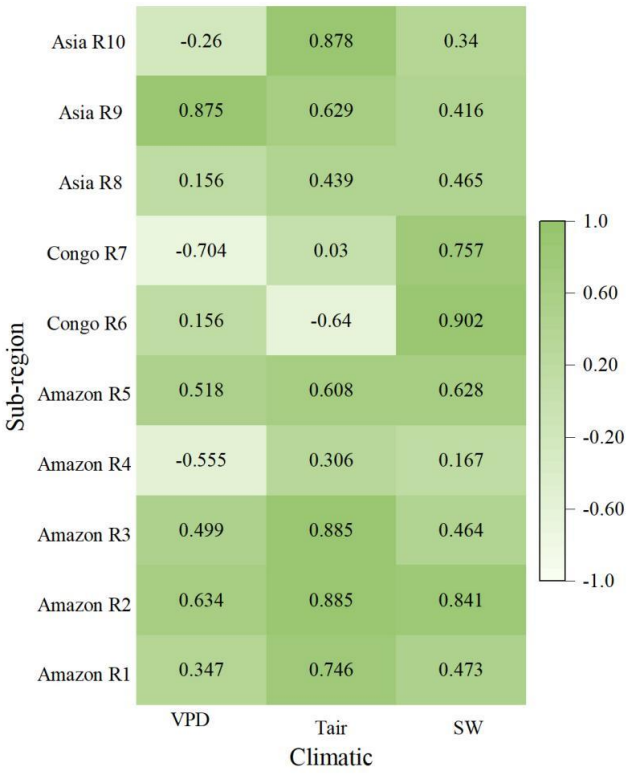

Figure S6. The correlation coefficients (R) between the young leaf $V_{c,max25}$ and climatic in ten regions classified using K-means method.

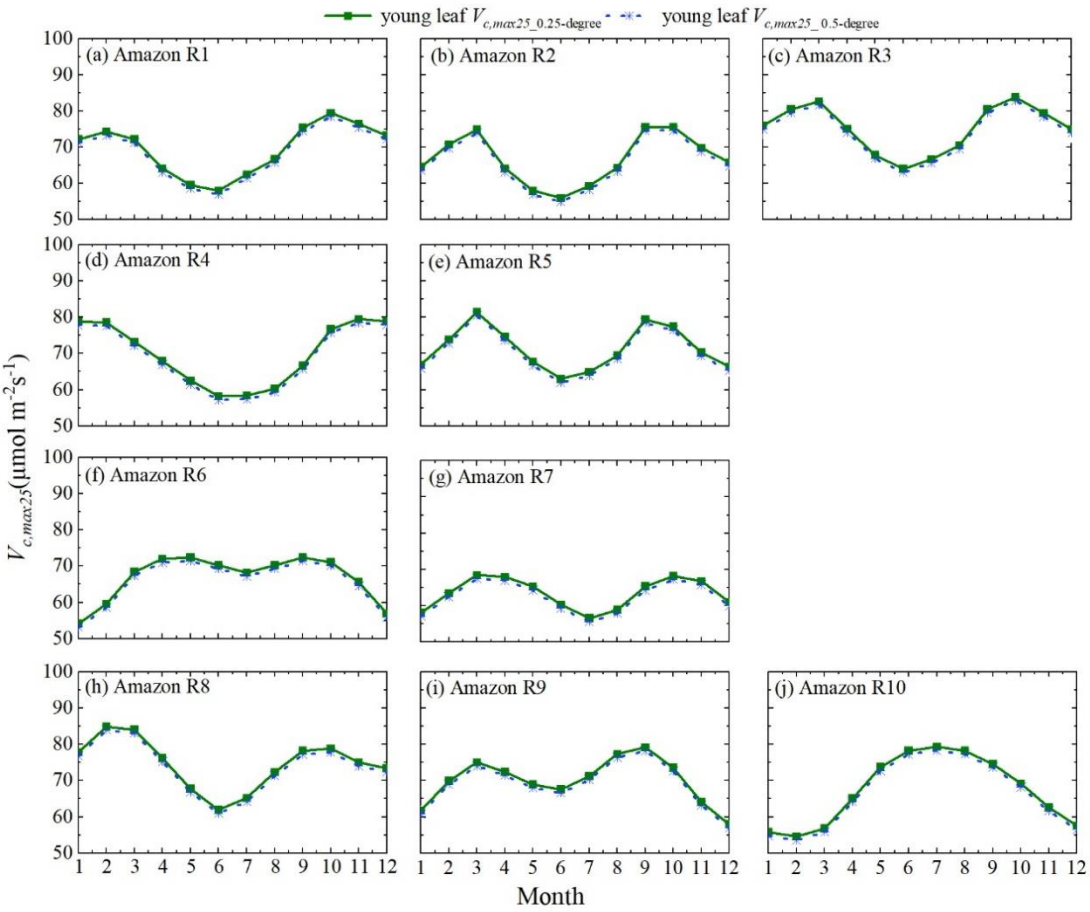

Figure S7. Comparation the seasonality of young leaf $V_{c,max25}$ leaves at 0.25° and 0.5° scale in the ten clustered regions.

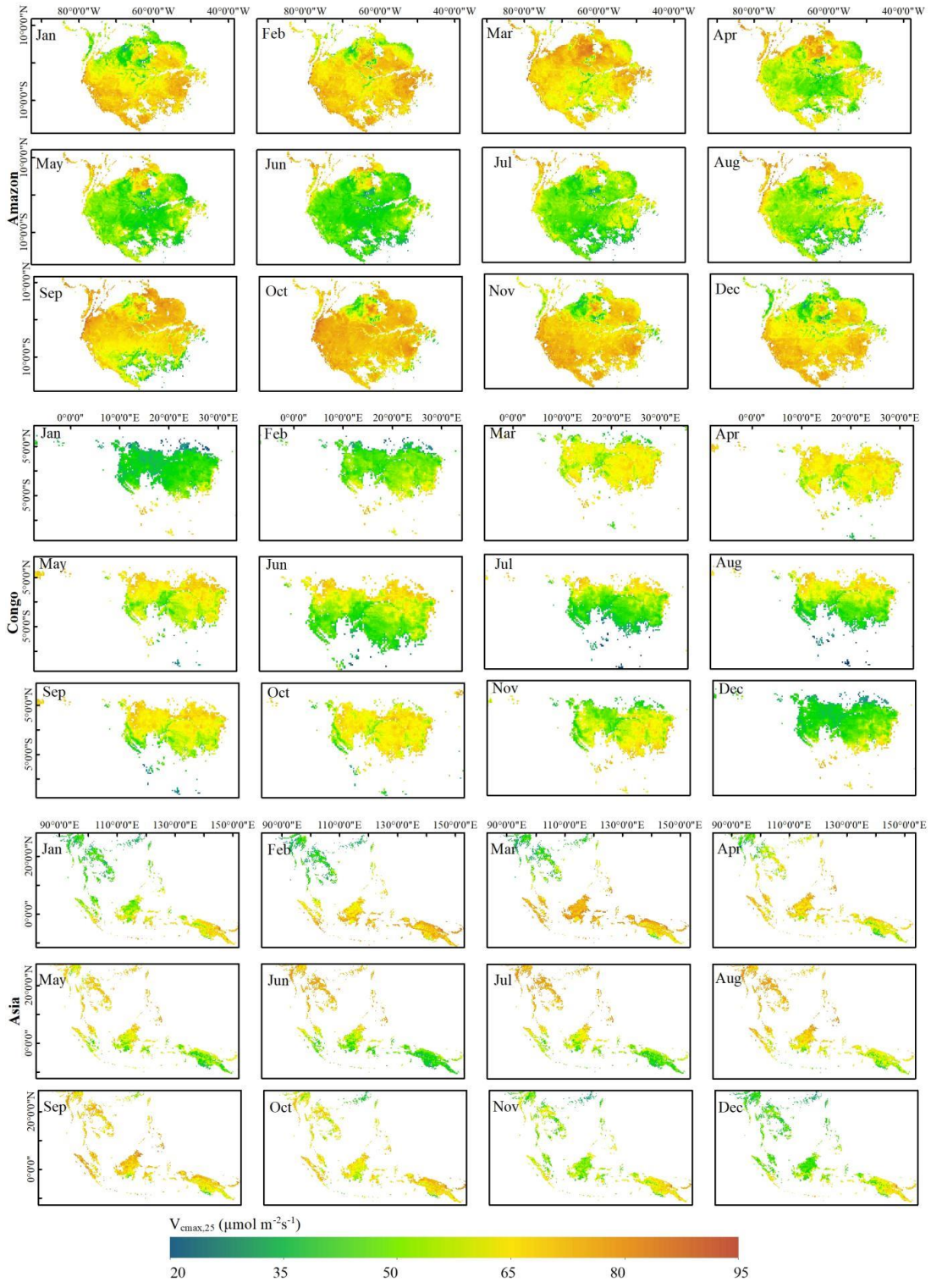

Figure S8. Spatial distributions and seasonal changes of young leaf $V_{c,max25}$ in TEFs derived from RT-SIF (2001–2018). White areas are missing data.

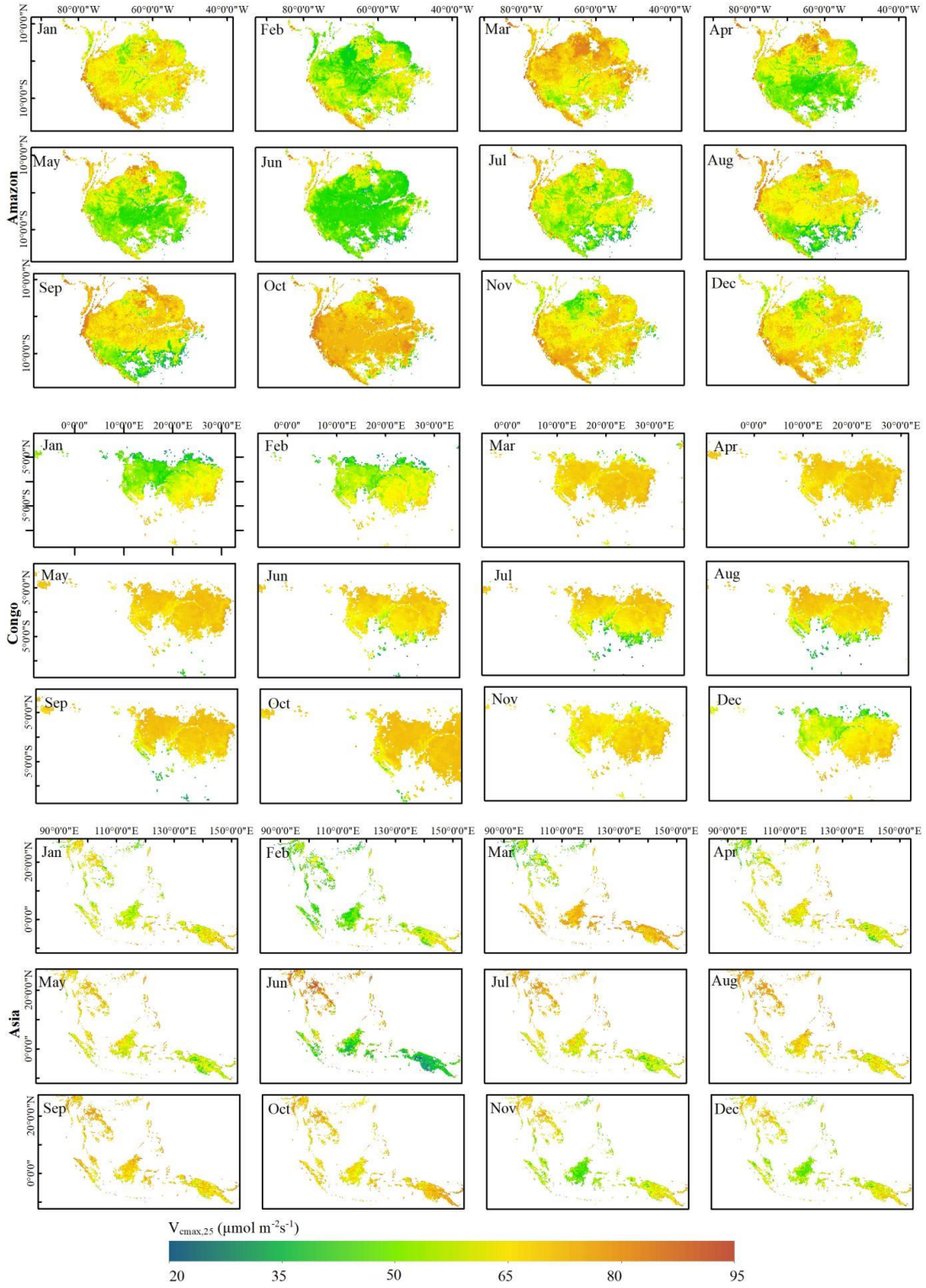

Figure S9. Spatial distributions and seasonal changes of young leaf $V_{c,max25}$ in TEFs derived from Go-SIF (2001–2018). White areas are missing data.

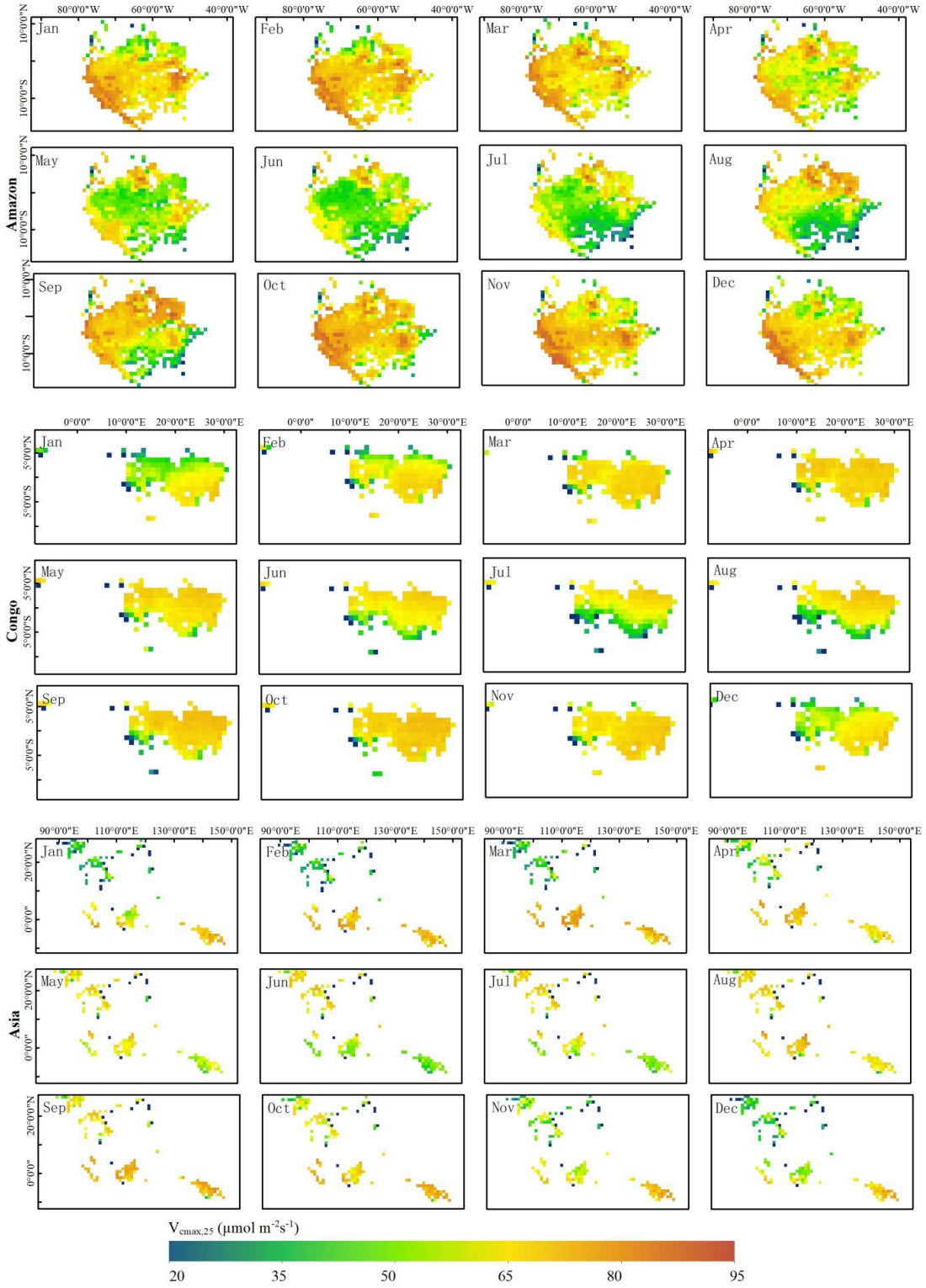

Figure S10. Spatial distributions and seasonal changes of young leaf $V_{c,max25}$ in TEFs derived from FLUXCOM (2001–2013). White areas are missing data. Black dots are invalid value.

Supplementary Tables

Table S1 In situ observation sites information of $V_{c,max25}$ from previously published literatures

Site name	**Lat**	**Lon**	$V_{c,max25}$	**References**
BR-Sa1	2.8567°S	54.958°W	young and mean leaves age $V_{c,max25}$	Keller et al., 2004
GF-Guy	5.278°N	52.925°W	mean leaves age $V_{c,max25}$	Wang et al., 2022
CN-Din	23.170°N	112.540°E	mean leaves age $V_{c,max25}$	https://fluxnet.org/data/fluxnet2015-dataset/
MDJ-03	5.984°S	12.869°E	mean leaves age $V_{c,max25}$	Ishida et al., 2015

Table S2 Information of four sites with observations of eddy covariance data

Site ID	Site Name	Latitude	Longitude
AU-Rob	Robson Creek, Queensland, Australia Forest Ecosystem Research Station	-17.12	145.63
BR-Sa1	Santarem-Km67-Primary Forest Ecosystem Research Station	-2.86	-54.96
BR-Sa3	Santarem-Km83-Logged Forest Ecosystem Research Station	-3.02	-54.97
GF-Guy	Guyaflux (French Guiana) Forest Ecosystem Research Station	5.28	-52.92

Table S3 Information of total LAI mean values from previously published literatures

NO.	LAI mean	Sites	Methods	References
1	5.88	K34	observation	Wu et al., 2016
2	5.89	K67	observation	Wu et al., 2016
3	5.7	K67	observation	Smith et al., 2019
4	5.34	Congo	observation	de Wasseige et al., 2003
5	5.93	Xishuangbanna	observation	Li et al., 2010
6	6.0	ORCHIDEE TrBE module	Module	De Weirdt et al., 2012
7	5.45	Tapajo´s National Fores	observation	Asner et al., 2003
8	6.04	Barro Colorado Island	observation	Wirth et al., 2001
9	6.0	Costa Rican Forest	observation	Clark et al., 2008
10	5.9	Tapajo´s National Forest	observation	Brando et al., 2008
11	5.67	Dinghushan	observation	Zhao, Chen et al., 2020

Table S4-Part1 Equations of photosynthesis and stomatal conductance model for calculating An, Ac, Aj and Ap and intermediate variables in Figure 2

Equations	**Notes**	**Ref.**
$A_n = \min\left\{A_c, A_j, A_p\right\} - R_{dark}$	Net carbon assimilation rate (A_n, μmol/m^2/s).	Farquhar et al., 1980; Bernacchi et al., 2013
$A_c = V_{c\max} \times \frac{c_i - \Gamma^*}{c_i + K_C \times (1 + \frac{O}{K_O})}$	Rubisco-limited photosynthetic rate (w_c, μmol/m^2/s)	Farquhar et al., 1980
$A_j = J \times \frac{c_i - \Gamma^*}{4 \times (c_i + 2 \times \Gamma^*)}$	Electron-transport lim ted rate of photosynthetic rate (w_j, μmol/m^2/s)	Farquhar et al., 1980
$J = \frac{J_e + J_{\max} - \sqrt{(J_e + J_{\max})^2 - 4 \times \Theta \times J_e \times J_{\max}}}{2 \times \Theta}$	The rate of electrons through the thylakoid membrane (μmol/m^2/s)	Farquhar et al., 1980; Bernacchi et al., 2013
$J_e = Q \times \alpha \times \beta \times \Phi_{PSII}$	The rate of whole electron transport provided by light (μmol/m^2/s).	Bernacchi et al., 2013
$A_p = 0.5 \times V_{c\max}$	Triose phosphate expor t limited rate of photosynthesis (μmol/m^2/s)	Ryu et al., 2011
$Para = Para_{25} \times \exp(\frac{(T_K - 298.15) \times \Delta H_{para}}{R \times T_K \times 298.15})$	Temperature dependence function for various parameters including K_C, K_O , Γ^* , R_{dark} and V_{cmax}. T_K denotes leaf temperature in Kelvin. Reference temperature is 25 ℃.	Bernacchi et al., 2013
$J_{\max} = J_{\max,25} \times \exp((\frac{25 - T_{opt}}{\Omega_T})^2 - (\frac{T_K - 273.15 - T_{opt}}{\Omega_T})^2)$	Temperature dependence frunction for maximum electron transport rate (J_{max}). T_{opt} is the optimal temperature for $J_{max.}$	Bernacchi et al., 2013; June et al., 2004
$g_s = 1.6 \times (1 + \frac{g_1}{\sqrt{VPD}}) \times \frac{A_n}{c_a}$ $A_n = g_s \times (c_a - c_i)$ $\Rightarrow c_i = c_a \times (1 - \frac{1}{1.6 \times (1 + \frac{g_1}{\sqrt{VPD}})})$	Use optimal stomatal model to estimate internal CO_2 concentration (c_i) from atmospheric CO_2 concentration (c_a) and vapor pressure deficit (VPD)	Lin et al., 2015; Medlyn et al., 2011

Table S4-Part2 Parameters used in photosynthesis and stomatal conductance model for calculating An, Ac, Aj and Ap and intermediate variables in Figure 2

Symbol/Equations	**Notes**	**Ref.**
$c_a = 380$	Atmospheric CO_2 concentration (ppm)	
$g_1 = 3.77$	Coefficient in stomatal conductance scheme	Lin et al., 2015
$J_{\max,25} = 1.67 \times V_{c\max,25}$	Maximum electron transport rate (μmol/m^2/s) at 25 ℃	Medlyn et al., 2002
$O = 210$	Atmospheric O_2 concentration (pp thousand)	
$R = 8.314$	Universal gas constant (J/K/mol)	
$T_{opt} = 35$	Optimal temperature for J_{max} (℃)	Lloyd and Farquhar, 2008
$K_{C,25} = 404.9$ $\Delta H_{K_C} = 79.43$	Michaelis-Menton constant for carboxylase (μmol/mol) at 25 ℃ and activation energy for temperature dependence (kJ/mol)	Bernacchi et al., 2001
$K_{O,25} = 278.4$ $\Delta H_{K_O} = 36.38$	Michaelis-Menton constant for oxygenase (mmol/mol) at 25 ℃ and activation energy for temperature dependence (kJ/mol)	Bernacchi et al., 2001
$R_{dark,25} = 0.015 \times V_{c\max,25}$ $\Delta H_{R_{dark}} = 46.39$	Leaf dark respiration (μmol/m^2/s) at 25 ℃ and activation energy for temperature dependence (kJ/mol)	Bernacchi et al., 2001
$V_{c\max,25}$ $\Delta H_{V_{c\max}} = 65.33$	Maximum carboxylation rate (μmol/m^2/s) at 25 ℃ is acquired from observations. Its activation energy for temperature dependence (kJ/mol) is listed	Bernacchi et al., 2001
$\Gamma^*_{25} = 42.75$ $\Delta H_{\Gamma^*} = 38.83$	CO_2 compensation point (μmol/mol) at 25 ℃ and activation energy for temperature dependence (kJ/mol)	Bernacchi et al., 2001
$\alpha = 0.85$	Leaf absorbance fraction of photosynthetically active radiation (PAR)	Farquhar et al., 1980; Bernacchi et al., 2013
$\beta = 0.5$	Fraction of PAR that reaches PSII system	Farquhar et al., 1980; Bernacchi et al., 2013
$\Phi_{PSII} = 0.352 + 0.022 \times T_{℃} - 3.42e^{-4}T_{℃}$	Maximum quantum efficiency of PSII photochemistry. $T_{℃}$ denotes leaf temperature in Celsius.	Bernacchi et al., 2003; Evans, 1989; von Caemmerer et al., 2000
$\Theta = 0.76 + 0.018 \times T_{℃} - 3.7e^{-4}T_{℃}$	Convexity of light-response curve. $T_{℃}$ denotes leaf temperature in Celsius.	Bernacchi et al., 2003; Evans, 1989; Ögren and Evans, 1993
$\Omega_T = 11.6 + 0.18 \times T_{opt}$	Coefficient for the temperature function of J_{max}.	Bernacchi et al., 2003

Table S4-Part3 An, Ac, Aj and Ap and intermediate variables in Figure 2. Equations to calculate radiative transfer within canopy with a total leaf area index as LAI_{total}

Equations	**Notes**	**Ref.**
$Q_{tot} = (1-\rho_{cb}) \times PAR_{b,0} \times (1-e^{-k_b' \times CI \times L_C}) + (1-\rho_{cd}) \times PAR_{d,0} \times (1-e^{-k_d' \times CI \times L_C})$	Total PAR absorbed by canopy (μmol/m^2/s)	He et al., 2012; Ryu et al., 2011; De Pury and Farquhar, 1997
$k_b = \frac{0.5}{\cos(SZA)}$	Extinction coefficient for sun-lit fraction of LAI	De Pury and Farquhar, 1997
$k_b' = \frac{0.46}{\cos(SZA)}$	Extinction coefficient for beam and scattered beam PAR	De Pury and Farquhar, 1997
$k_d' = 0.719$	Extinction coefficient for diffuse and scattered diffuse PAR	De Pury and Farquhar, 1997
$\rho_{cb} = 0.029$	Canopy reflection coefficient for beam PAR	De Pury and Farquhar, 1997
$\rho_{cd} = 0.036$	Canopy reflection coefficient for diffuse PAR	De Pury and Farquhar, 1997
$\sigma = 0.15$	Leaf scatting coefficient of radiation	De Pury and Farquhar, 1997
$CI = 0.63$	Leaf clumping index	De Pury and Farquhar, 1997

Table S4-Part4 Equations to calculate incoming photosynthetically active radiation (PAR) over canopy

Equations	**Notes**	**Ref.**
$PAR_{b,0} = R_{short} \times f_{PAR} \times f_{PAR,b}$ $PAR_{d,0} = R_{short} \times f_{PAR} \times (1 - f_{PAR,b})$	The canopy top photosynthetically active radiation in beam ($PAR_{b,0}$) and diffuse ($PAR_{d,0}$) light	Weiss and Norman, 1985
$f_{PAR} = \frac{R_{b,vis} + R_{d,vis}}{R_{b,nir} + R_{d,nir} + R_{b,vis} + R_{d,vis}}$ $f_{PAR,b} = \frac{R_{b,vis}}{R_{b,vis} + R_{d,vis}} \times (1 - (\frac{0.9 - \frac{R_{short}}{R_{b,nir} + R_{d,nir} + R_{b,vis} + R_{d,vis}}}{0.7})^2)$	The fraction of total PAR over total incoming radiation (f_{PAR}) and the fraction of beam PAR over total PAR ($f_{PAR,b}$)	Weiss and Norman, 1985
$R_{b,vis} = \frac{600 \times e^{-0.185 \times \frac{P}{P_0} \times m}}{m}$	Expected beam visible radiation under clear sky (W/m^2)	Weiss and Norman, 1985
$R_{d,vis} = \frac{0.4 \times (600 - R_{b,vis} \times m)}{m}$	Expected diffuse visible radiation under clear sky (W/m^2)	Weiss and Norman, 1985
$R_{b,nir} = \frac{720 \times e^{-0.06 \times \frac{P}{P_0} \times m} - w}{m}$	Expected beam near-infrared radiation under clear sky (W/m^2)	Weiss and Norman, 1985
$R_{d,nir} = \frac{0.6 \times (720 - R_{b,nir} \times m - w)}{m}$	Expected diffuse near-infrared radiation under clear sky (W/m^2)	Weiss and Norman, 1985
$w = 1320 \times 10^{-1.195 + 0.4459 \times \log_{10} m - 0.0345 \times (\log_{10} m)^2}$	Expected water absorbance of near-infrared radiation in the atmosphere (W/m^2)	Weiss and Norman, 1985
$m = \cos(SZA)^{-1}$	Parameter calculated from solar zenith angle (SZA)	Weiss and Norman, 1985

References

Asner, G.P., Scurlock, J.M.O. and A. Hicke, J.: Global synthesis of leaf area index observations: implications for ecological and remote sensing studies, Global Ecol. Biogeogr., 12, 191-205, 10.1046/j.1466-822X.2003.00026.x, 2003.

Bernacchi, C. J., Singsaas, E. L., Pimentel, C., Portis Jr, A. R., and Long, S. P.: Improved temperature response functions for models of Rubisco-limited photosynthesis, Plant, Cell Environ., 24, 253-259, 10.1111/j.1365-3040.2001.00668.x, 2001.

Bernacchi, C. J., Pimentel, C., and Long, S. P.: In vivo temperature response functions of parameters required to model RuBP-limited photosynthesis, Plant, Cell Environ., 26, 1419-1430, 10.1046/j.0016-8025.2003.01050.x, 2003.

Bernacchi, C. J., Bagley, J. E., Serbin, S. P., Ruiz-Vera, U. M., Rosenthal, D. M., and Vanloocke, A.: Modelling C3 photosynthesis from the chloroplast to the ecosystem, Plant, Cell Environ., 36, 1641-1657, 10.1111/pce.12118, 2013.

Brando, P. M., Nepstad, D. C., Davidson, E. A., Trumbore, S. E., Ray, D. and Camargo, P.: Drought effects on litterfall, wood production and belowground carbon cycling in an Amazon forest: Results of a throughfall reduction experiment, Philos. T. R. Soc. B., 363, 1839-1848, 10.1098/rstb.2007.0031, 2008.

Chen, Z. H., Zhang, H. T., and Wang, B. S.: Studies on biomass and production of the lower subtropical evergreen broad-leaved forest in Heishiding Natural Reserve, VII. Litterfall, litter standing crop and litter decomposition rate, Journal of Tropical and Subtropical Botany, 107-114, http://europepmc.org/abstract/CBA/539457, 1992.

Clark, D.B., Olivas, P.C., Oberbauer, S.F., Clark, D.A. and Ryan, M.G.: First direct landscape-scale measurement of tropical rain forest Leaf Area Index, a key driver of global primary productivity, Ecol. Lett., 11, 163-172, 10.1111/j.1461- 0248.2007.01134.x, 2008.220

De Pury, D. G. G. and Farquhar, G. D.: Simple scaling of photosynthesis from leaves to canopies without the errors of big-leaf models, Plant, Cell Environ., 20, 537-557, 10.1111/j.1365-3040.1997.00094.x, 1997.

de Wasseige, C., Bastin, D. and Defourny, P.: Seasonal variation of tropical forest LAI based on field measurements in Central African Republic, Agr. Forest Meteorol., 119, 181-194, 10.1016/S0168-1923(03)00138-2, 2003.

Evans, J. R.: Photosynthesis and Nitrogen Relationships in Leaves of C_3 Plants, Oecologia, 78, 9-19, jstor.org/stable/4218825, 1989.

Farquhar, G. D., von Caemmerer, S., and Berry, J. A.: A biochemical model of photosynthetic

CO2 assimilation in leaves of C3 species, Planta, 149, 78-90, 10.1007/BF00386231, 1980.

He, L., Chen, J. M., Pisek, J., Schaaf, C. B., and Strahler, A. H.: Global clumping index map derived from the MODIS BRDF product, Remote Sens. Environ., 119, 118-130, 10.1016/j.rse.2011.12.008, 2012.

Ishida, F. Y., Feldpausch, T. R., Grace, J., Meir, P. W., Saiz, G., Séné, O., Lloyd, J., 2015. Biome-specific effects of nitrogen and phosphorus on the photosynthetic characteristics of trees at a forest-savanna boundary in Cameroon, 178(3): 659-672.

June, T., Evans, J. R., and Farquhar, G. D.: A simple new equation for the reversible temperature dependence of photosynthetic electron transport: a study on soybean leaf, Funct. Plant Biol., 31, 275-283, 10.1071/FP03250, 2004.

Keller, M., Alencar, A., Asner, G. P., Braswell, B., Bustamante, M., Davidson, E., Vourlitis, G. L., 2004. Ecological research in the large-scale biosphere–atmosphere experiment in Amazonia: early results. Ecological Applications, 14(sp4):3-16.

Li, Z., Zhang, Y., Wang, S., Yuan, G., Yang, Y. and Cao, M.: Evapotranspiration of a tropical rain forest in Xishuangbanna, southwest China, Hydrol. Process., 24, 2405-2416, 10.1002/hyp.7643, 2010.

Lin, Y.-S., Medlyn, B. E., Duursma, R. A., Prentice, I. C., Wang, H., Baig, S., Eamus, D., de Dios, Victor R., Mitchell, P., Ellsworth, D. S., de Beeck, M. O., Wallin, G., Uddling, J., Tarvainen, L., Linderson, M.-L., Cernusak, L. A., Nippert, J. B., Ocheltree, T. W., Tissue, D. T., Martin-StPaul, N. K., Rogers, A., Warren, J. M., De Angelis, P., Hikosaka, K., Han, Q., Onoda, Y., Gimeno, T. E., Barton, C. V. M., Bennie, J., Bonal, D., Bosc, A., Löw, M., Macinins-Ng, C., Rey, A., Rowland, L., Setterfield, S. A., Tausz-Posch, S., Zaragoza-Castells, J., Broadmeadow, M. S. J., Drake, J. E., Freeman, M., Ghannoum, O., Hutley, Lindsay B., Kelly, J. W., Kikuzawa, K., Kolari, P., Koyama, K., Limousin, J.-M., Meir, P., Lola da Costa, A. C., Mikkelsen, T. N., Salinas, N., Sun, W., and Wingate, L.: Optimal stomatal behaviour around the world, Nat. Clim. Change, 5, 459-464, 10.1038/nclimate2550, 2015.

Lloyd, J. and Farquhar, G. D.: Effects of rising temperatures and [CO2] on the physiology of tropical forest trees, Philos. T. R. Soc. B., 363, 1811-1817, 10.1098/rstb.2007.0032, 2008.

Medlyn, B. E., Duursma, R. A., Eamus, D., Ellsworth, D. S., Prentice, I. C., Barton, C. V. M., Crous, K. Y., De Angelis, P., Freeman, M., and Wingate, L.: Reconciling the optimal and empirical approaches to modelling stomatal conductance, Glob. Change Biol., 17, 2134-2144, 10.1111/j.1365-2486.2010.02375.x, 2011.

Medlyn, B. E., Dreyer, E., Ellsworth, D., Forstreuter, M., Harley, P. C., Kirschbaum, M. U. F., Le Roux, X., Montpied, P., Strassemeyer, J., Walcroft, A., Wang, K., and Loustau, D.: Temperature response of parameters of a biochemically based model of photosynthesis. II. A review of experimental data, Plant, Cell Environ., 25, 1167-1179, 10.1046/j.1365-3040.2002.00891.x, 2002.

Melton, J., Shrestha, R., and Arora, V.: The influence of soils on heterotrophic respiration exerts a strong control on net ecosystem productivity in seasonally dry Amazonian forests, Biogeosciences, 11, 1151-1168, 10.5194/bgd-11-12487-2014, 2014.

Ögren E. and Evans J.R.: Photosynthetic light-response curves. I. The influence of CO2 partial pressure and leaf inversion, Planta, 189, 180-190, 1993.

Ryu, Y., Jiang, C., Kobayashi, H., and Detto, M.: MODIS-derived global land products of shortwave radiation and diffuse and total photosynthetically active radiation at 5 km resolution from 2000, Remote Sens. Environ., 204, 812-825, 10.1016/j.rse.2017.09.021, 2018.

Ryu, Y., Baldocchi, D. D., Kobayashi, H., van Ingen, C., Li, J., Black, T. A., Beringer, J., van Gorsel, E., Knohl, A., Law, B. E., and Roupsard, O.: Integration of MODIS land and atmosphere products with a coupled-process model to estimate gross primary productivity and evapotranspiration from 1 km to global scales, Global Biogeochem. Cy., 25, n/a-n/a, 10.1029/2011gb004053, 2011.

Sharma, E. and Ambasht, R. S.: Litterfall, Decomposition and Nutrient Release in an Age Sequence of Alnus Nepalensis Plantation Stands in the Eastern Himalaya, J. Ecol., 75, 10.2307/2260309, 1987.

Smith, M. N., Stark, S. C., Taylor, T. C., Ferreira, M. L., de Oliveira, E., Restrepo-Coupe, N., Chen, S., Woodcock, T., dos Santos, D. B., Alves, L. F., Figueira, M., de Camargo, P. B., de Oliveira, R. C., Aragão, L. E. O. C., Falk, D. A., McMahon, S. M., Huxman, T. E. and Saleska, S. R.: Seasonal and drought-related changes in leaf area profiles depend on height and light environment in an Amazon forest. New Phytol., 222, 1284-1297, 10.1111/nph.15726, 2019.

Weiss, A. and Norman, J. M.: Partitioning solar radiation into direct and diffuse, visible and near-infrared components, Agr. Forest Meteorol., 34, 205-213, 10.1016/0168- 1923(85)90020-6, 1985.

Wirth, R., Weber, B., and Ryel, R. J.: Spatial and temporal variability of canopy structure in a tropical moist forest, Acta Oecol., 22(5-6), 2001.

Wu, J., Albert, L. P., Lopes, A. P., Restrepo-Coupe, N., Hayek, M., Wiedemann, K. T., Guan, K., Stark, S. C., Christoffersen, B., Prohaska, N., Tavares, J. V., Marostica, S., Kobayashi, H., Ferreira, M. L., Campos, K. S., da Silva, R., Brando, P. M., Dye, D. G., Huxman, T. E., Huete, A. R., Nelson, B. W., and Saleska, S. R.: Leaf development and demography explain photosynthetic seasonality in Amazon evergreen forests, Science, 351, 972-976, 10.1126/science.aad5068, 2016.

Zhao, Y., Chen, X., Smallman, T. L., Flack-Prain, S., Milodowski, D. T., and Williams, M.: Characterizing the Error and Bias of Remotely Sensed LAI Products: An Example for Tropical and Subtropical Evergreen Forests in South China, Remote Sens., 12, 3122, 10.3390/rs12193122, 2020.